Copy
RM L53E29

NACA RM L53E29

RESEARCH MEMORANDUM
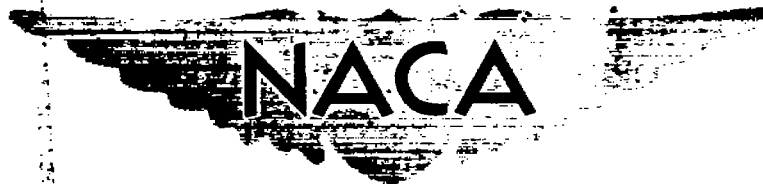
UNCLASSIFIED

To_____

By authority of NASA ltr dtd Mar. 12, 1964, s/ F. George Drobka
TAR-4.9

DRAG MEASUREMENTS AT LOW LIFT OF A FOUR-NACELLE AIRPLANE

CONFIGURATION HAVING A LONGITUDINAL DISTRIBUTION

OF CROSS-SECTIONAL AREA CONDUCIVE TO LOW

TRANSONIC DRAG RISE

By Russell N. Hopko, Robert O. Piland,
and James R. Hall

Langley Aeronautical Laboratory
Langley Field, Va.

NATIONAL ADVISORY COMMITTEE
FOR AERONAUTICS
WASHINGTON
November 18, 1953

NATIONAL ADVISORY COMMITTEE FOR AERONAUTICS

RESEARCH MEMORANDUM

DRAG MEASUREMENTS AT LOW LIFT OF A FOUR-NACELLE AIRPLANE

CONFIGURATION HAVING A LONGITUDINAL DISTRIBUTION

OF CROSS-SECTIONAL AREA CONDUCIVE TO LOW

TRANSONIC DRAG RISE

By Russell N. Hopko, Robert O. Piland,
and James R. Hall

SUMMARY

A procedure based on the transonic area rule has been used to design a four-nacelle delta-wing airplane configuration. A flight test of a model of the configuration showed a zero-lift transonic drag rise of 0.010 which, when compared with estimates, indicated the absence of adverse interference effects. A body of revolution having the same longitudinal distribution of cross-sectional area as the configuration was also flight tested and its measured transonic drag rise agreed with that of the configuration, thereby confirming the validity of the transonic drag rule for a complex aircraft configuration.

INTRODUCTION

The development of high-speed aircraft has been hampered by the high pressure drag encountered at transonic and supersonic speeds. In many cases these high drag levels are not the result of poorly designed components, but rather the result of adverse interference effects created when the components are combined in a configuration. In an attempt to resolve the problem, recourse has been made to the transonic area rule of reference 1. The rule states that near the speed of sound the zero-lift drag rise of a wing-body configuration usually should be mainly dependent on the axial distribution of cross-sectional areas normal to the airstream.

References 1 and 2 present results of investigations which verify the area rule for certain wing-body combinations. The purpose of the present investigation is to extend the use of the area rule to the design

of a low-drag four-nacelle airplane configuration and in so doing to confirm the validity of the rule for more complex configurations.

This paper presents the method used in designing the aforementioned aircraft and the results of drag tests of the configuration and the equivalent body of revolution. These results were obtained from rocket tests of the configuration over a Mach number range of 0.8 to 1.35, corresponding to a Reynolds number range of 6×10^6 to 20×10^6 based on the wing mean aerodynamic chord, and helium gun tests of a 1/5.5-scale equivalent body of revolution between Mach numbers of 0.8 and 1.27, corresponding to a Reynolds number range of 6×10^6 to 9×10^6 based on body length. The tests were conducted at the Langley Pilotless Aircraft Research Station at Wallops Island, Va.

DESIGN PROCEDURE

As mentioned in the introduction, the transonic area rule states that the transonic drag rise of a configuration is mainly dependent upon its longitudinal distribution of cross-sectional area. It was reasoned, therefore, that if an airplane configuration were designed having the same distribution of cross-sectional area as a body of revolution, it should have practically the same pressure drag near a Mach number of 1 as the body. It was also believed that the good longitudinal distribution of area of the airplane should be derived from well-designed components; that is, the rule would tend to break down if the components are of a shape that will cause boundary-layer separation. A parabolic body of fineness ratio 9, known to have low drag on the basis of previous free-flight tests (ref. 3 and some unpublished data) and theoretical calculations, was selected. The body contour is shown in figure 1 with its defining equation and its area distribution. The area distributions of the wing, engines, and vertical tails were calculated. These components were selected as typical of an aircraft of this type. By superimposing the area distribution of the components on the area distribution of figure 1 a fuselage may be defined. In order to keep the selected components fair it was necessary to depart somewhat from the desired area distribution. The area distribution of the configuration is shown in figure 2(a). The area distribution and the equivalent body of revolution of the configuration in nondimensional form are compared with the basic parabolic body in figure 2(b).

CONFIGURATIONS AND TESTS

The airplane configuration (model 1) is shown in figure 3. Photographs of the model are presented as figure 4. The model was of composite

magnesium-wood construction with the nacelles made of Fiberglas-Paraplex laminate. Model 2 (fig. 5) is a 1/5.5-scale equivalent body of revolution of model 1. (A photograph of the model is shown as fig. 6.) The cross-sectional area of the stabilizing fins was subtracted from that of the body. The model was constructed of aluminum alloy.

Model 1 was rocket boosted and Model 2 was catapulted to Mach numbers of 1.35 and 1.27, respectively. During the coasting period that followed, velocity and flight-path data for the rocket model were obtained by means of radar. These data were reduced to values of drag coefficient and Mach number by techniques described in reference 4. Corrections to the data were made for the effects of winds at altitude. The variation of Reynolds number with Mach number is shown in figure 7. The total errors are estimated to be within the following limits:

Mach number, M . . . . ±0.01

Drag coefficient, C_D . . . . ±0.001

RESULTS AND DISCUSSION

The drag at low lift of the aircraft configuration is shown in figure 8(a) with an estimate of the internal drag of the four nacelles. Shown also is an estimate of the drag of the configuration obtained by summing the estimated drags of the individual components. The rather low pressure drag rise of 0.010 is gratifying in itself; the comparison of the estimated and measured drag, however, seems to be of even more import, the implication being that adverse interference effects may be minimized by utilizing a relatively simple design procedure based on the area-rule concept.

Figure 8(b) presents the measured zero-lift drag of the body of revolution (fig. 6) having the same longitudinal distribution of area as the aircraft configuration. Figure 9 presents a comparison of the pressure drag increment of this body and the aircraft configuration with a Mach number of 0.95 selected as the drag-rise Mach number. The agreement shows the validity of the area rule when applied to rather complex configurations.

Comparison of the pressure drag rise of the parabolic body (fig. 1), estimated from data presented in references 3 and 5 and from some unpublished data, and the equivalent body of the aircraft configuration shows appreciable difference (fig. 9). This difference may be attributed to differences in the longitudinal area distribution as shown in figure 2 and emphasizes the need to have the area distribution of the configuration match that of the basic body closely.

CONCLUDING REMARKS

The transonic area rule has been used in an attempt to design a four-nacelle aircraft configuration having low transonic and supersonic pressure drag. Models of the configuration and its equivalent body of revolution were flight tested. The following conclusions were drawn from the tests which were at low lift:

1. By using a simple design procedure based on the transonic area rule, rather complex aircraft configurations having low transonic and supersonic pressure drags may be designed. For the configuration designed during this investigation a drag rise of 0.01 was measured.

2. The transonic area concept applies to rather complex configurations as is shown by the agreement between the pressure drag of the configuration and its equivalent body of revolution.

3. Relatively small deviations from an optimum distribution may result in significant increases in pressure drag rise.

Langley Aeronautical Laboratory,
    National Advisory Committee for Aeronautics,
        Langley Field, Va., May 13, 1953.

REFERENCES

1. Whitcomb, Richard T.: A Study of the Zero-Lift Drag-Rise Character-
     istics of Wing-Body Combinations Near the Speed of Sound. NACA
     RM L52H08, 1952.

2. Robinson, Harold L.: A Transonic Wind-Tunnel Investigation of the
     Effects of Body Indentation, as Specified by the Transonic Drag-Rise
     Rule, on the Aerodynamic Characteristics and Flow Phenomena of a
     45° Sweptback-Wing—Body Combination. NACA RM L52L12, 1953.

3. Hart, Roger G., and Katz, Ellis R.: Flight Investigations at High-
     Subsonic, Transonic, and Supersonic Speeds To Determine Zero-Lift
     Drag of Fin-Stabilized Bodies of Revolution Having Fineness Ratios
     of 12.5, 8.91, and 6.04 and Varying Positions of Maximum Diameter.
     NACA RM L9I30, 1949.

4. Welsh, Clement J.: Results of Flight Tests To Determine the Zero-Lift
     Drag Characteristics of a 60° Delta Wing With NACA 65-006 Airfoil
     Section and Various Double-Wedge Sections at Mach Numbers From 0.7
     to 1.6. NACA RM L50F01, 1950.

5. Fraenkel, L. E.: The Theoretical Wave Drag of Some Bodies of Revolu-
     tion. Rep. No. Aero 2420, British R.A.E., May 1951.
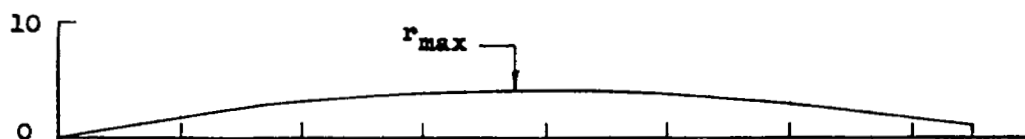
$$\text{Forebody} \quad \frac{r}{r_{max}} = 1 - 4\left[0.5 - \frac{x}{1125}\right]^2$$

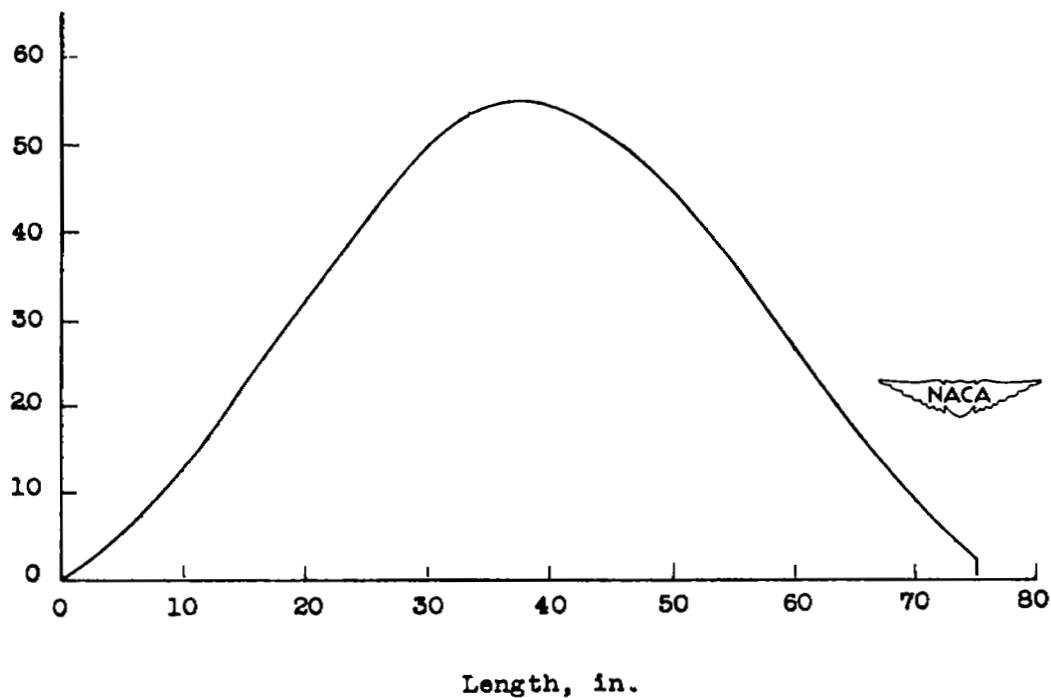$$\text{Afterbody} \quad \frac{r}{r_{max}} = 1 - 3.2\left[\frac{x}{1125} - 0.5\right]^2$$
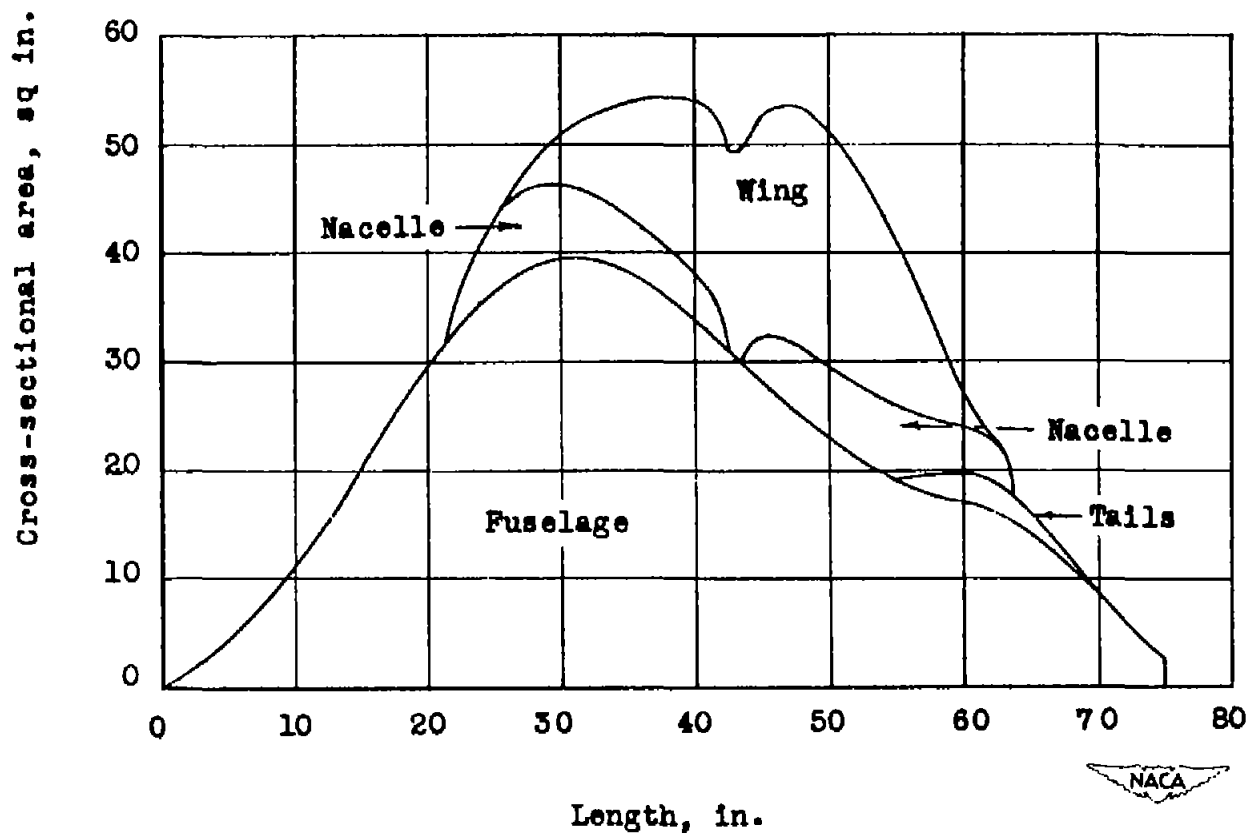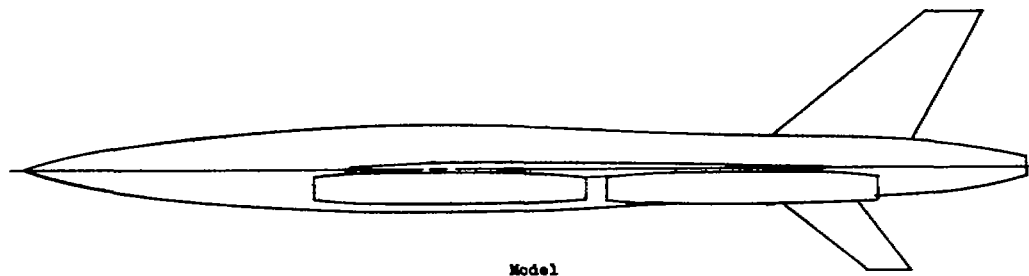
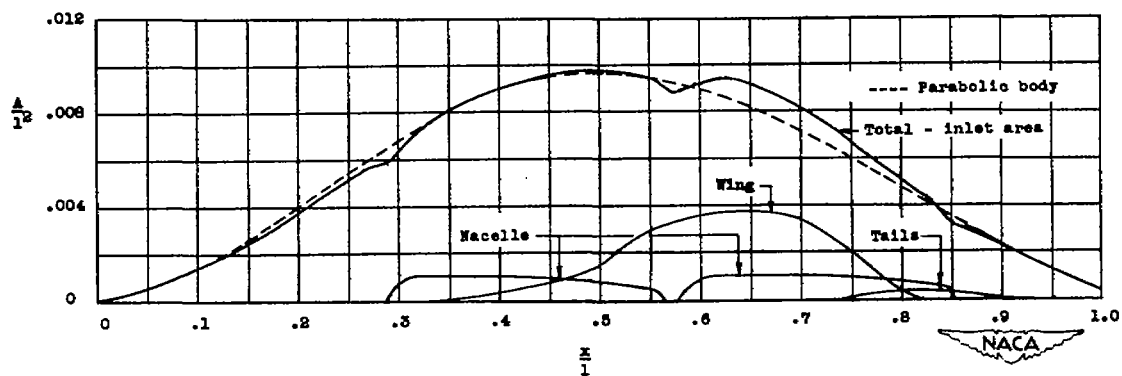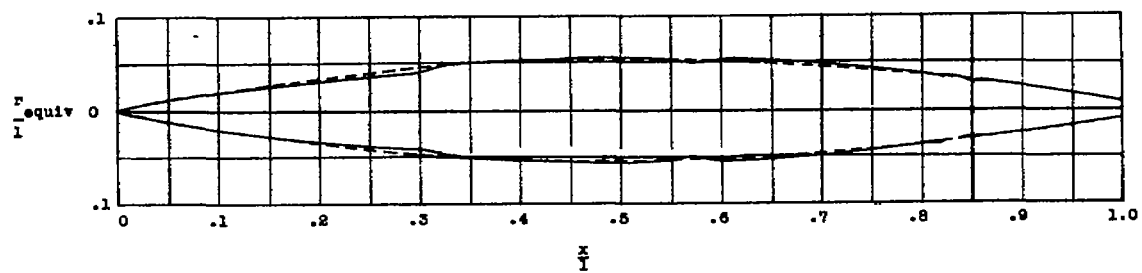Figure 1.- Full-scale parabolic body.

(a) Dimensional.

Figure 2.- Longitudinal area distribution.

Model

Equivalent body l/d_{max} = 8.95
Parabolic body l/d_{max} = 9.00

(b) Nondimensional

Figure 2.- Concluded.

Fuselage Coordinates			
X	Y	X	Y
0	0	37.00	3.435
1.00	0.208	39.00	3.340
2.00	.428	41.00	3.225
3.00	.645	43.00	3.100
5.00	1.037	45.00	2.972
7.00	1.405	47.00	2.847
9.00	1.744	49.00	2.733
11.00	2.059	51.00	2.636
13.00	2.359	53.00	2.557
15.00	2.610	55.00	2.490
17.00	2.835	57.00	2.432
19.00	3.035	59.00	2.377
21.00	3.202	61.00	2.319
23.00	3.341	63.00	2.257
25.00	3.440	65.00	2.189
27.00	3.511	67.00	2.032
29.00	3.548	69.00	1.819
31.00	3.558	71.00	1.524
33.00	3.544	73.00	1.182
35.00	3.502	75.00	.833

Nacelle Coordinates					
x'	R_o	R_1	x'	R_o	R_1
0	0.845	0.845	12.614	1.300	1.050
.281	.920	.853	12.947	1.299	1.049
.414	.948	.857	13.281	1.297	1.047
.614	.988	.862	13.614	1.287	1.037
.947	1.050	.872	14.281	1.280	1.030
1.281	1.103	.882	14.947	1.261	1.011
1.614	1.151	.901	15.614	1.235	.986
1.947	1.191	.941	16.281	1.203	.973
2.281	1.226	.976	16.947	1.165	.935
2.614	1.254	1.004	17.614	1.120	.910
2.947	1.275	1.025	18.281	1.068	.878
3.281	1.290	1.040	18.947	1.010	.867
3.614	1.298	1.048	19.281	.979	.867
3.861	1.300	1.050	19.614	.948	.867
5.000	1.300	1.050	19.947	.911	.867
9.000	1.300	1.050	20.349	.867	.867

x' Nacelle station
R_o Outside radius of nacelle
R_1 Inside radius of nacelle

Wing sections are NACA 65A003

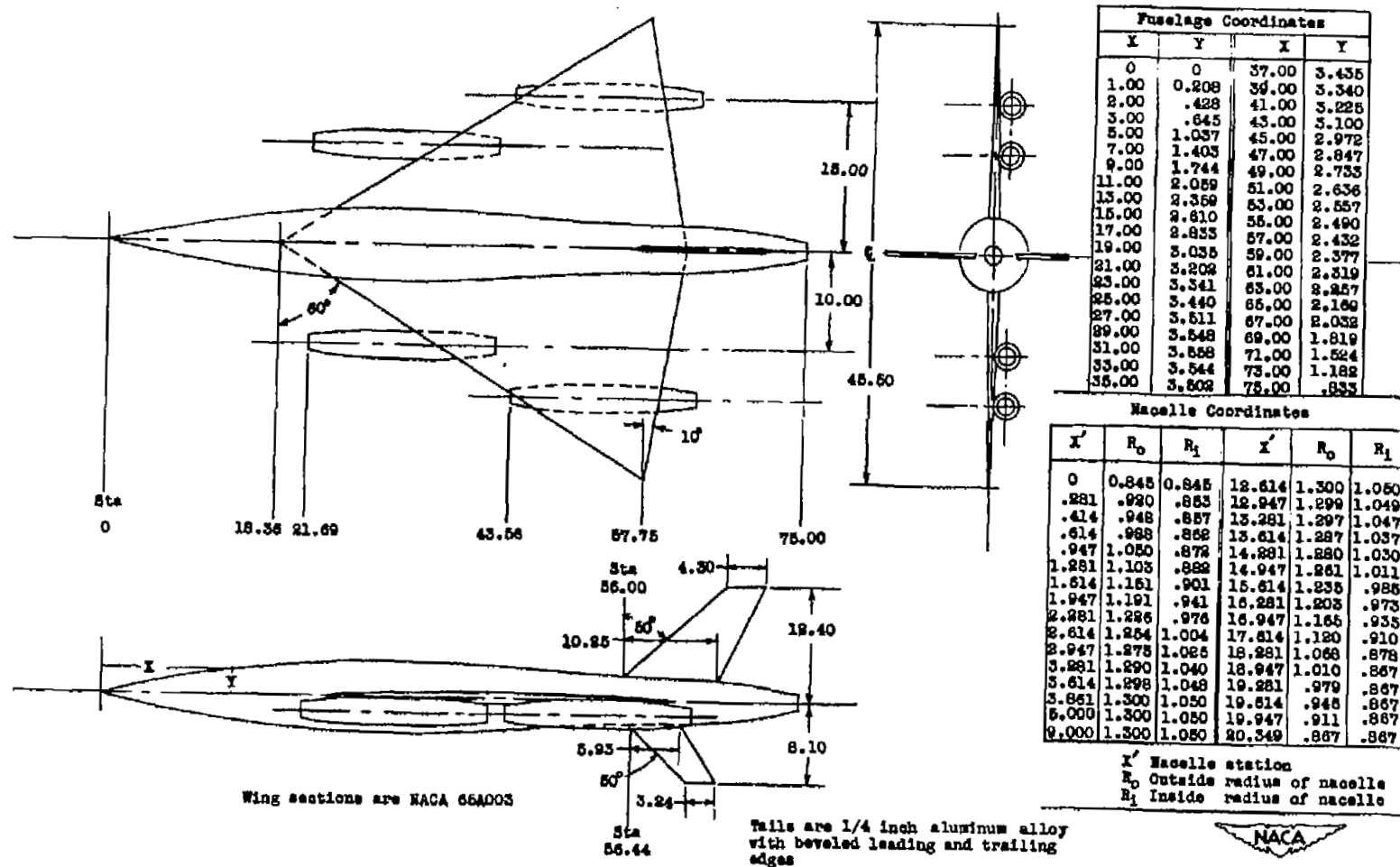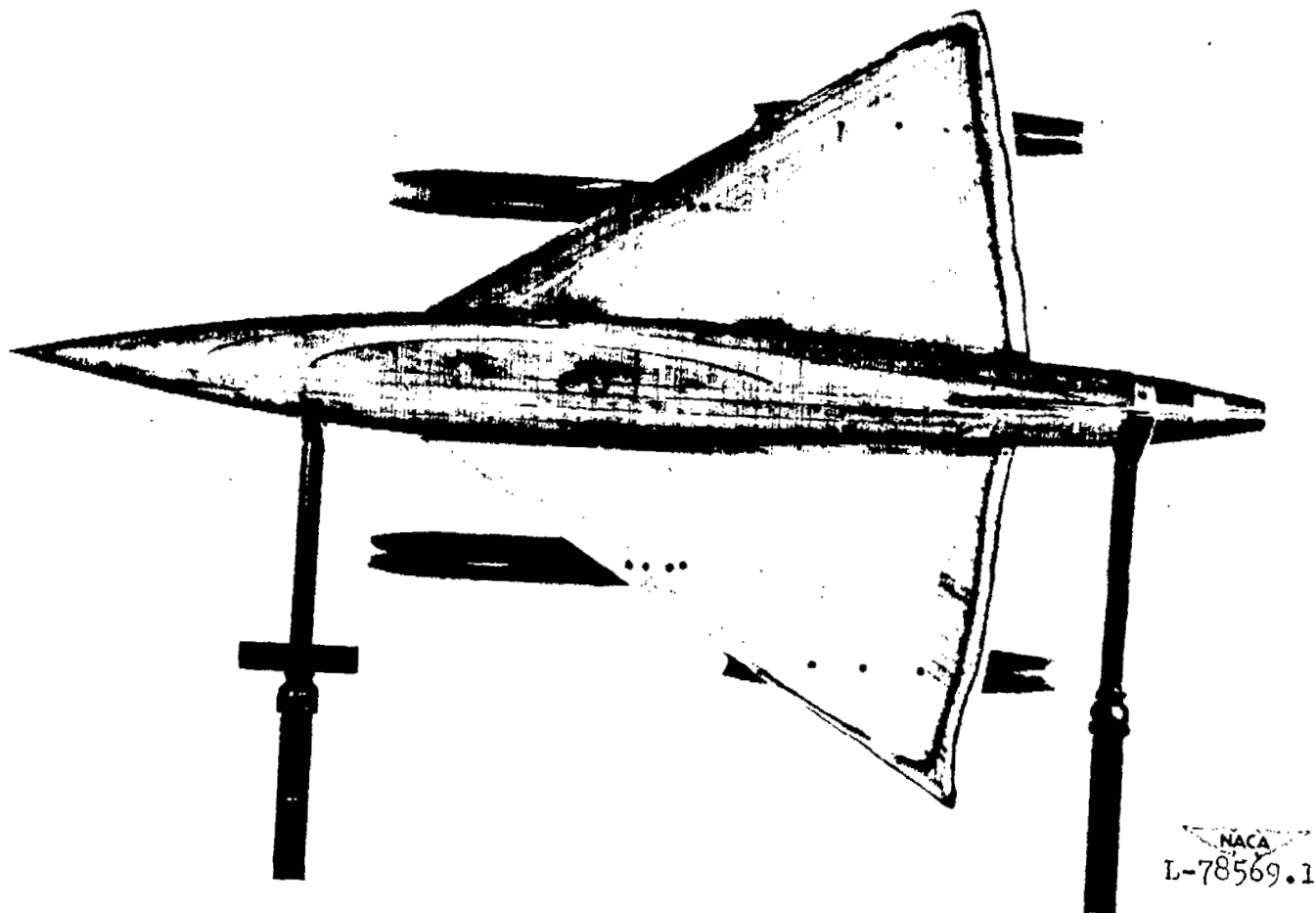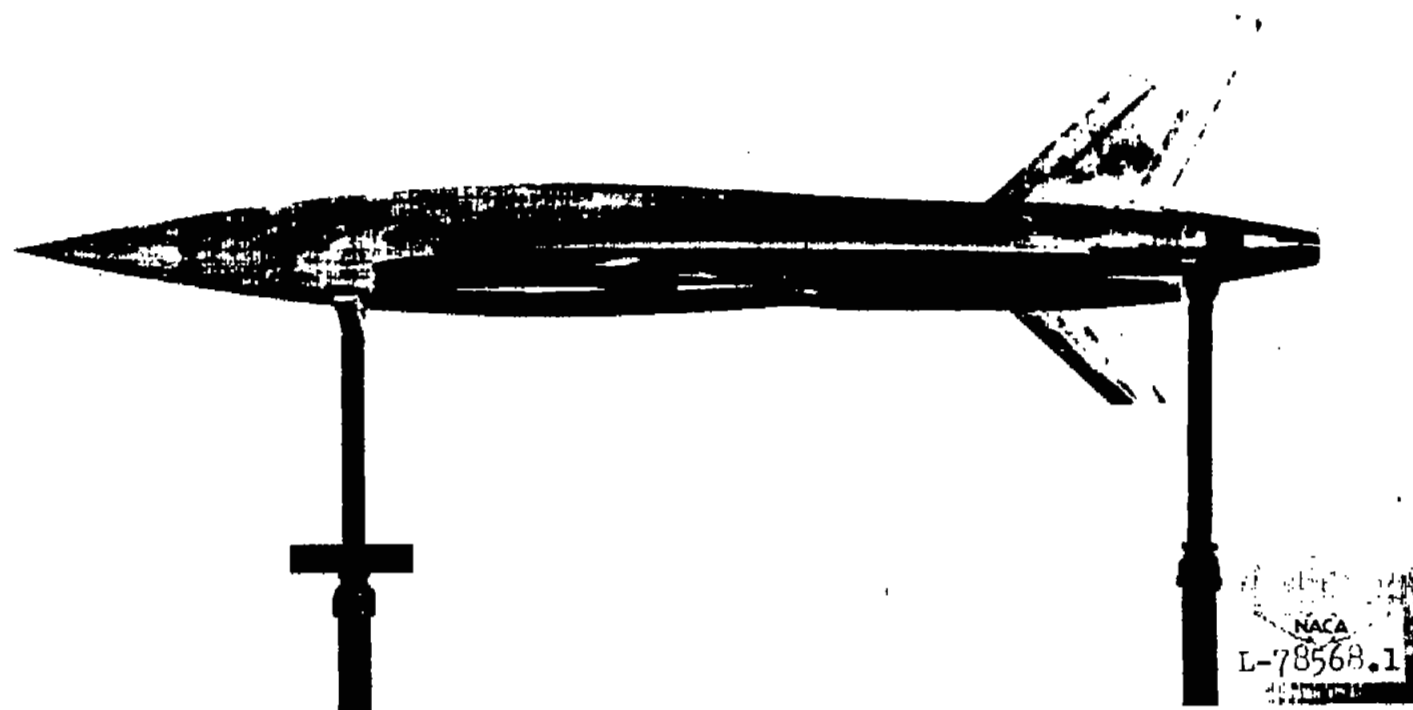Tails are 1/4 inch aluminum alloy with beveled leading and trailing edges

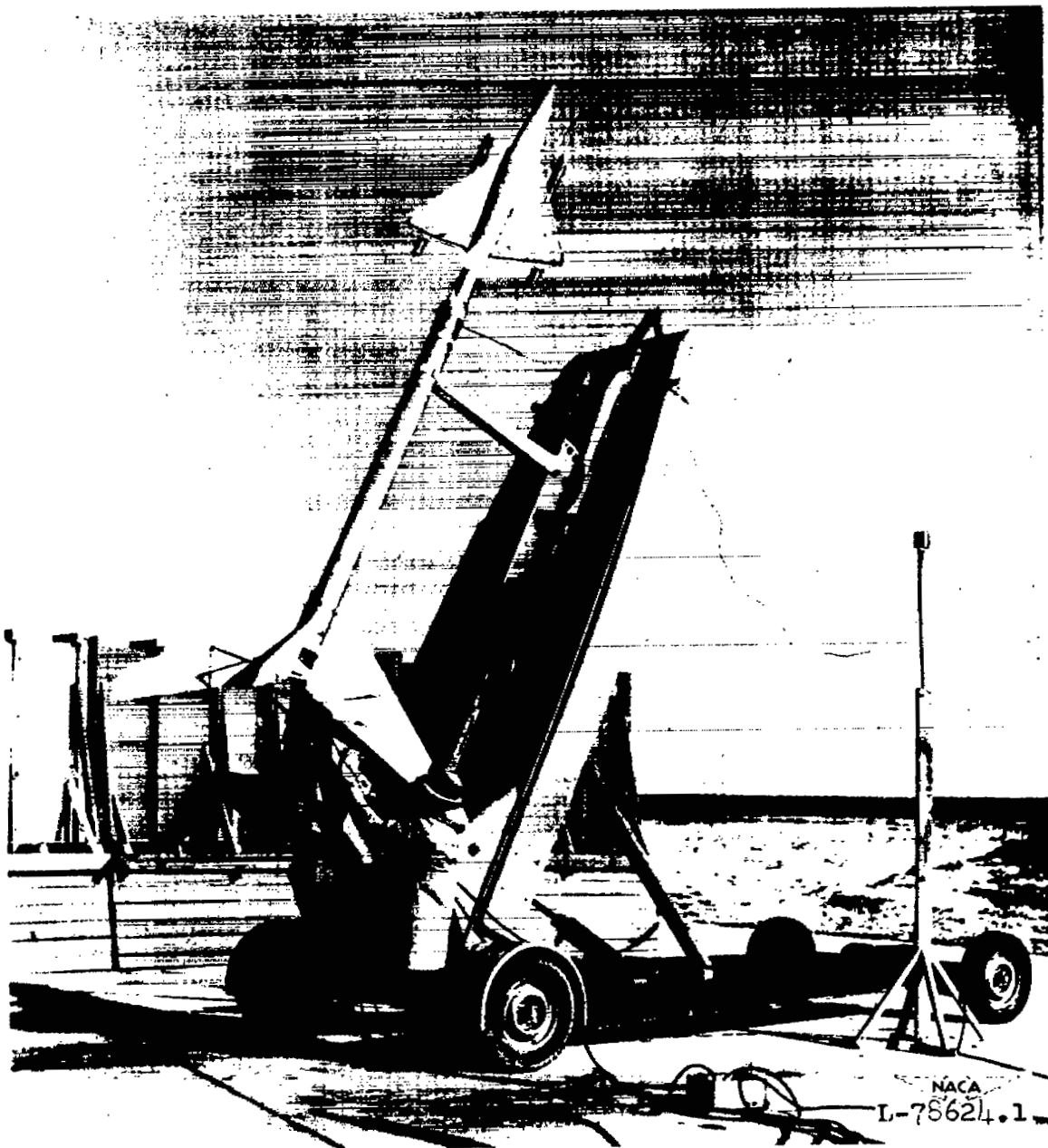Figure 3.- General arrangement of model 1. All dimensions in inches.

(a) Plan view.

Figure 4.- Model 1.

L-78569.1

(b) Side view.

Figure 4.- Continued.

(c) Model and booster on launcher.

Figure 4.- Concluded.

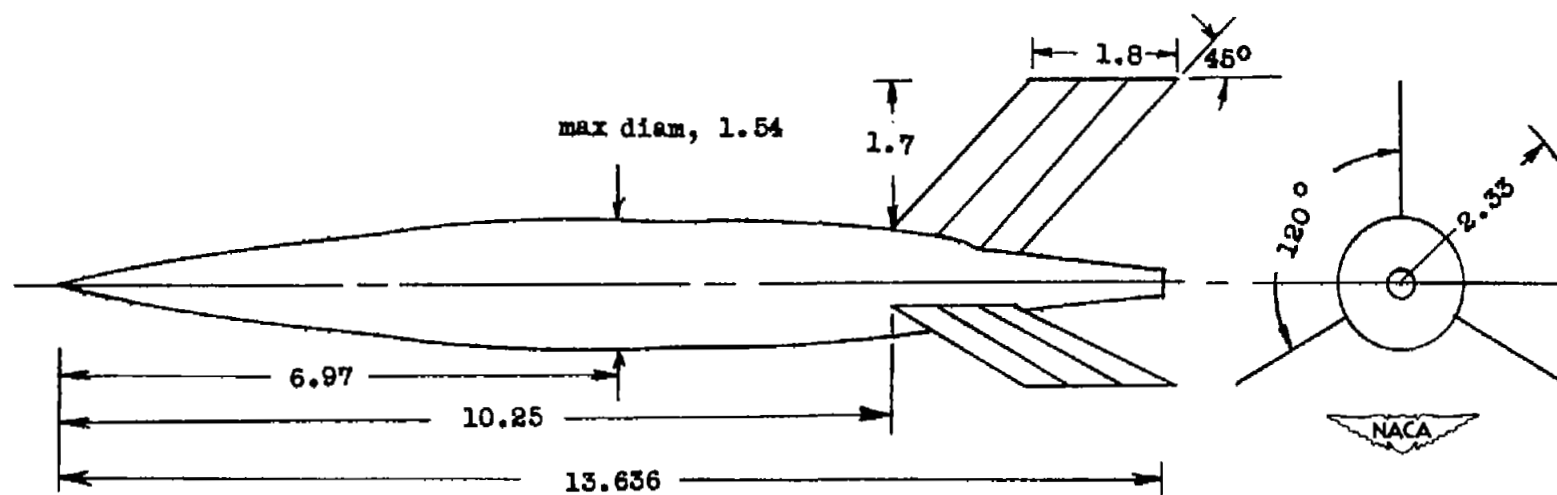max diam, 1.54

1.8

45°

1.7

120°

2.33

6.97

10.25

13.636

NACA

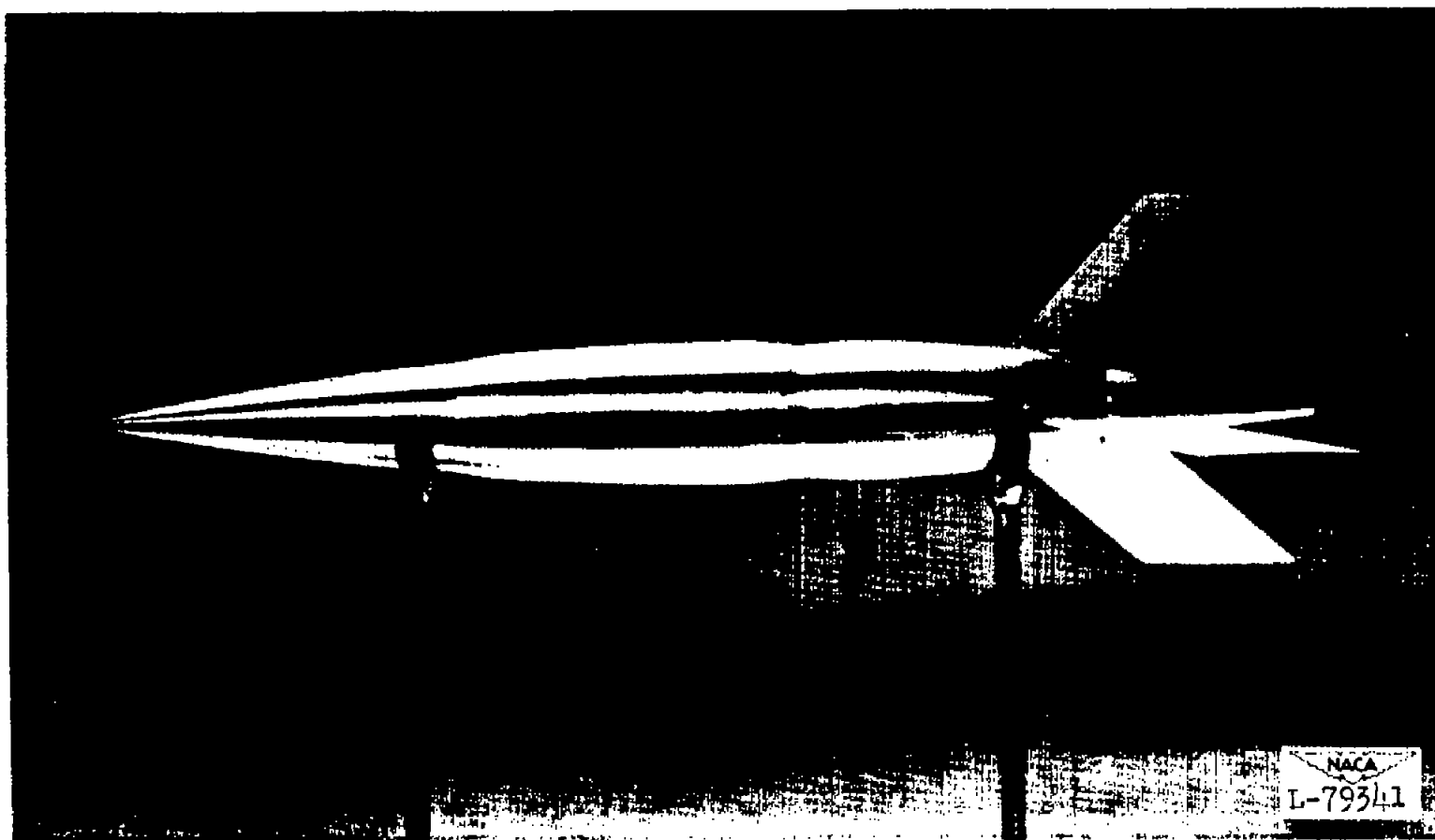Figure 5.- General arrangement of model 2. All dimensions in inches.
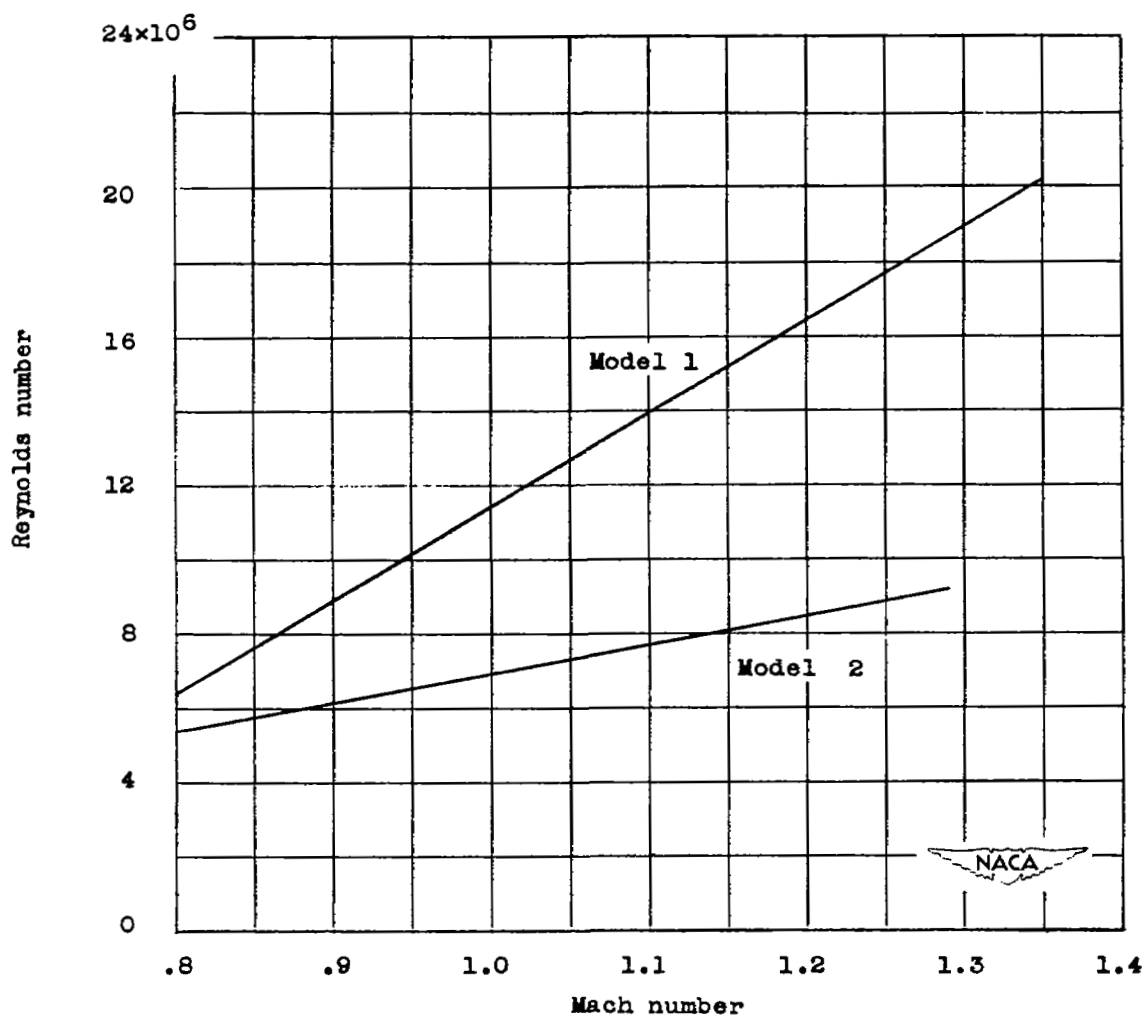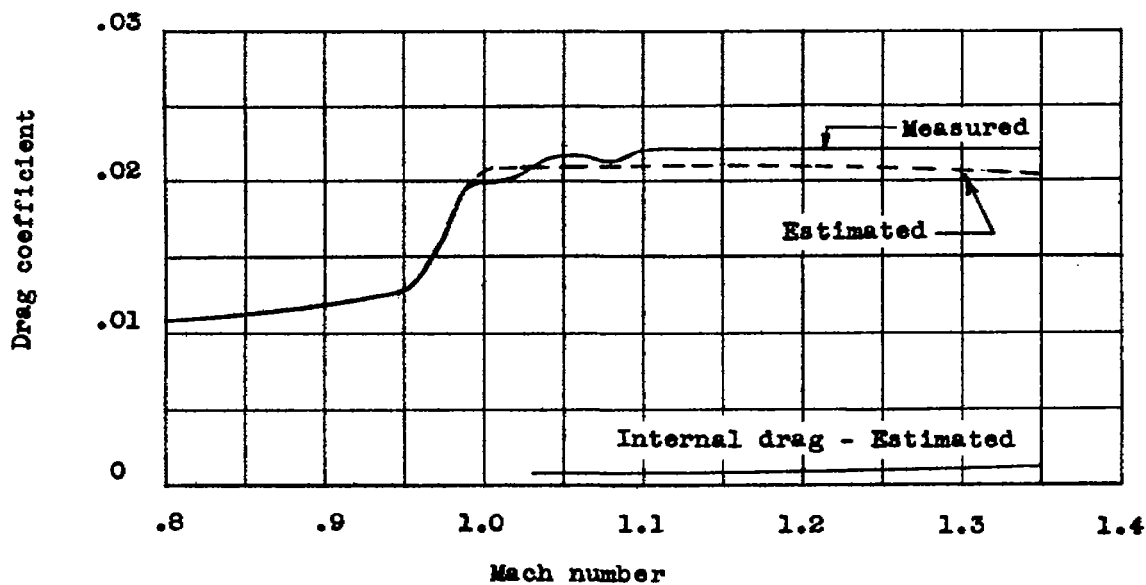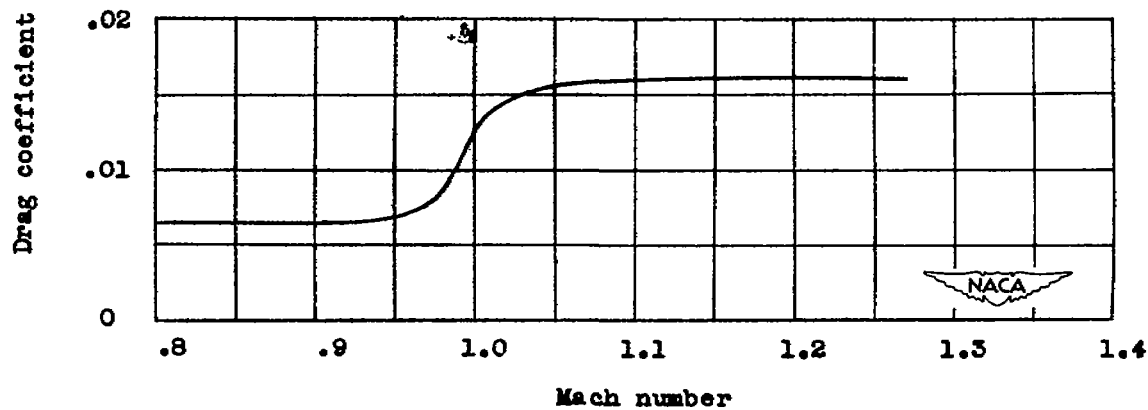
Figure 6.- Model 2.

Figure 7.- Variation of Reynolds number with Mach number based on wing
mean aerodynamic chord (model 1) and body length (model 2).

(a) Model 1.

(b) Model 2.

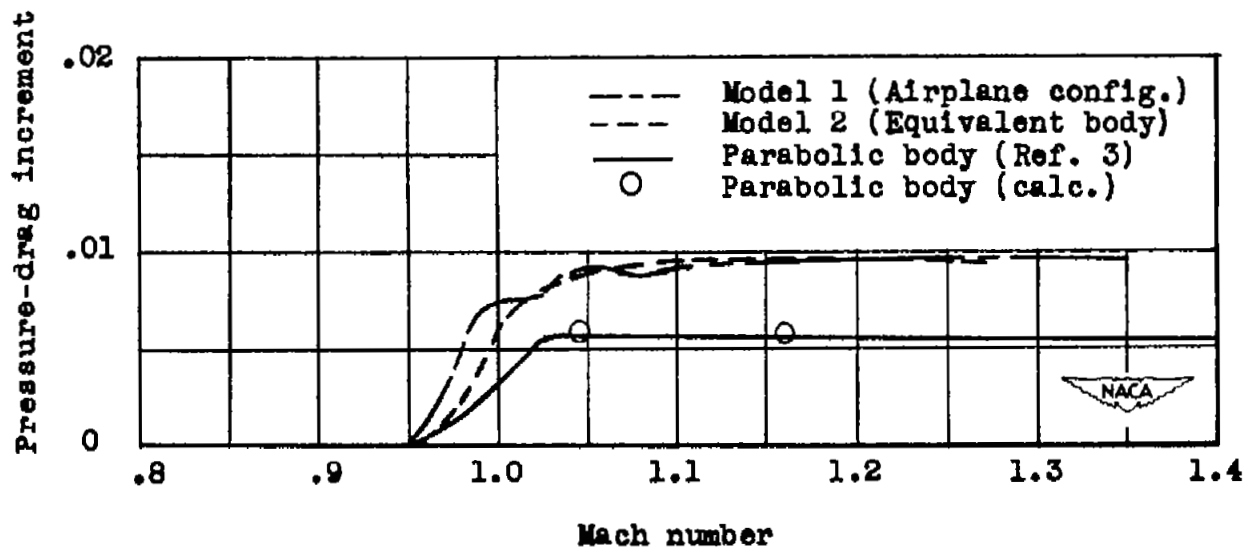Figure 8.- Variation of drag coefficient, based on wing area of airplane, with Mach number.

Figure 9.- Variation of pressure-drag increment with Mach number for models 1 and 2 and the parabolic body.